35th European and 10th International Conference on AE Testing
13th-16th September 2022 - Ljubljana, Slovenia

ACOUSTIC EMISSION APPLIED TO MODE I FATIGUE DAMAGE MONITORING OF ADHESIVELY BONDED JOINTS

Rosemere de Araujo Alves Lima[1], Andrea Bernasconi[1] and Michele Carboni[1,*]

[1]Dept. Mechanical Engineering, Politecnico di Milano – Via la Masa 1, 20156 Milano, Italy;
rosemere.dearaujo@polimi.it, andrea.bernasconi@polimi.it
*Correspondence: michele.carboni@polimi.it

ABSTRACT

The use of adhesively bonded joints has increased considerably due to their lightweight, relevant strength-weight ratio and possibility to join multi-materials. Nevertheless, there are still some challenges in the application of this kind of joints in primary structures, such as guaranteeing their reliability during the components' useful life.
Structural health monitoring methods are suggested to ensure in-service safety and reliability of adhesive joints. The acoustic emission appears promising because it can detect the elastic waves produced within the material when it is under damage or straining.
This research focuses on mode I fatigue damage monitoring metallic double cantilever beam adhesively bonded joints using the acoustic emission method. Digital image correlation and visual evaluation were applied during fatigue interruptions to track the crack-tip position within the adhesive and correlate them with the acoustic emission outcomes.
The acoustic emission method is susceptible and different kinds of waves (background, friction and damage) can be easily assessed during the tests, producing an immense amount of data. So, unsupervised artificial neural networks for patterning recognition were proposed. Self-organising maps and k-means algorithms were used for data clustering and then classified regarding their sources. Finally, the acoustic emission results, digital image correlation and visual evaluations were compared.

Keywords: Acoustic emission, adhesive joints, mode I fatigue, pattern recognition, clustering.

1. Introduction

The use of adhesively bonded joints has increased in recent years due to the global interest in producing lighter structures with the implementation of advanced multi-materials and the necessity of high-performance joining solutions for different types of interfaces. The adhesively bonded joints present the main advantage of producing low impact in the adherends mechanical properties, reducing stress concentration compared to traditional fasteners [1].
Nonetheless, the single use of adhesively bonded joints is still challenging for the application in primary structures since it is difficult to ensure joint reliability during a components in-service life, under fatigue and critical environmental conditions. To overcome these drawbacks and ensure the joint's integrity and safety, some solutions can be implemented, such as the enhancement of the adhesives' mechanical properties, development of optimized finite elements analysis to better

 https://doi.org/10.58286/27601

predict the joint's mechanical behaviour in critical loading-bearing conditions, and the use of Non-Destructive Testing (NDT) [2] Structural Health Monitoring (SHM) methods [3].
Since SHM methods can assess the joints' integrity under in-service life, giving the possibility of their on-demand or real-time diagnosis and prognostic, implementing a condition-based maintenance system that saves time and maintenance costs of the structures, the interest of the scientific community in their application is increasing.
Among the different SHM methods, Acoustic Emission (AE) is a promising alternative due to its possibility of assessing the elastic waves produced within the monitored material when their strain energy is released during the deformation or damage initiation and propagation (even in small increments) [4]. The assessed elastic waves are then recorded and have their time-domain features (i.e., amplitude, duration, counts, energy and rise time) and waveform saved by the acquisition system as detailed in the flowchart of Figure 1.

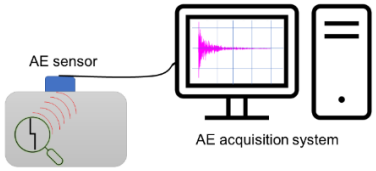

Figure 1: Flowchart of the acoustic emission system.

The AE method is susceptible also to background noise and elastic waves produced by friction within the material, recording a massive amount of data that requires a well-designed post-processing methodology for clustering and classifying the data related to damage sources from the ones related to noise. Time-domain or frequency-domain features filtering and, most recently, big-data algorithms such as supervised and unsupervised Artificial Neural Networks (ANN) are applied to clustering and AE sources classification.
The use of unsupervised ANN was applied in previous work to monitor the crack propagation within the bondline of metallic Double Cantilever Beam (DCB) specimens under quasi-static mode I crack propagation by using complementary algorithms (k-means and Self-Organised Maps) for the waveform's classification of the data related to the damage propagation from the background noise. In the same work, the AE results were compared with visual evaluation and Digital Image Correlation (DIC), where it was possible to localise the crack-tip position and the waveforms associated with the beginning of the onset of plasticisation ahead of the crack-tip (corresponding with the DIC outcomes). These interesting results can open new alternatives for using the AE method for monitoring adhesively bonded joints and help better understand the relationship between the AE signals and the damage mechanisms within the joints, possibly also under fatigue.
Only a few studies in the literature are dedicated to using the AE method for fatigue crack monitoring of adhesively bonded joints, particularly the relationship between the AE features and the damages mechanisms within the bondline [5]. J. A. Pascoe *et al*. 2018 [6], studied the use of acoustic emission to understand the fatigue crack growth within a single load cycle in adhesively bonded DCB joints. They focused on answering when damage occurs within single cycle fatigue tests, based on peak amplitude analyses of each signal. They could address the feasibility of this SHM method to monitor fatigue crack growth and its relationship with AE signals. However, still challenging to establish a well-defined link between the physical mechanisms correlated to the crack growth and the AE features and consequently do better filtering of the AE signals.
So, this work aims to study a clustering methodology based on unsupervised ANN using Self-Organised Maps (SOM) and k-means algorithms for classifying the AE signals assessed during mode I fatigue crack growth tests of metallic adhesively bonded DCB specimens. Principal Component Analysis (PCA) was also implemented to individuate the most significant time-domain, or frequency-domain AE features to be used during the clustering process. DIC and visual evaluation analysis were then performed to track the crack growth during the tests and compare them with the AE features.

2. Methodology

2.1 Materials and sample fabrication

DCB specimens were produced following the ASTM D3433, and dimensions are detailed in Figure 2 (a). The adherends were produced with a high-strength steel DIN 40CrMoMn7, and the 3M Scotch-Weld^{TM} 9323 B/A structural adhesive was used to join them, whose mechanical properties can be found in [7].

Before bonding, the adherends were sandblasted and cleaned with acetone to remove impurities and waxes. After that, a Teflon tape was applied at the beginning of the specimens to ensure a non-bonded region. Moreover, a razorblade was introduced to guarantee a sharp notch at the beginning of the specimens. Then, the adhesive was manually mixed and applied to the cleaned surface of the adherends from the razor blade until the free edge of the sample. A minimum adhesive thickness of 0.3 mm was ensured by adding a 2% weight of glass microspheres (250 – 300 µm of diameter) within the adhesive layer.

The specimens were cured in an oven for a total of 5.5 hours following three main steps: linear increase of the temperature until 65°C for 1.5h, followed by a hold at 65°C for two hours and, finally, a linear decrease of the temperature for two hours until the room temperature. For the present work, two specimens (S1 and S2) were tested with an initial crack length (a_0) equal to 65 mm.

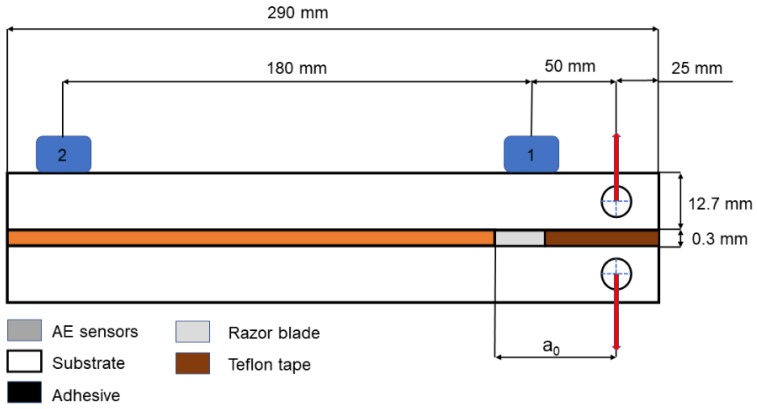

(a)

(b)

Figure 2: (a) DCB dimensions (drawings out of scale) and (b) testing setup.

For the crack growth measurement during the tests, both lateral surfaces of the specimens were previously whitely painted. The lateral surface used for the DIC analysis was furtherly painted using arbitrary black aerosol paint to create a fine speckle pattern.

2.2 Fatigue crack growth tests

A uni-axial MTS 810 servo-hydraulic testing machine with a load cell of 15 kN was used to perform mode I fatigue cracking growth tests. A constant amplitude load controlled test with a fatigue ratio (R = minimum load/maximum load) of 0.1. A testing frequency of 5 Hz and a maximum load equal to 850N was applied, as shown in Figure 2 (b).

The tests were interrupted every 5000 cycles to perform a monotonic loading ramp up to the maximum load applied during the fatigue cycles with a 0.5 mm/min speed rate. The maximum load was held for 10 seconds to allow crack length measurements by visual evaluation and DIC. After that, the machine unloads until the minimum load of the fatigue tests and the cycles then initiate again. The tests were performed until the specimen's complete failure.

A Dino-Lite digital microscope with a magnification of twenty times was used to take pictures of the white painted surface of the DCB specimens during the interruptions. The DIC analysis was made using the GOM – 3D Aramis adjustable system with an acquisition frequency of 3 Hz. The Aramis system's main characteristics are detailed in [8]. It is worth mentioning that the DIC acquisition system was synchronised with load and displacement input values from the testing machine.

The free post-processing software for image analysis FIJI – Image J (version 2020) and GOM Correlate (version 2020) were used for the visual evaluation and DIC pictures, respectively.

The acoustic emission analyses were performed during the cyclic and monotonic loading ramps using the Vallen ASMY-6 acquisition unit, two piezoelectric sensors units of type VS150-M (operating peak frequency in the range of 100 – 450 kHz) and a 34 dB Vallen AEP5 preamplifier, all connected by low-noise cables. Before the tests, a coupling silicon agent (OKS-110) was applied in the interface between samples and sensors to guarantee continuity during the AE signals transmission from the specimens to the acquisition system. The sensors were fixed on the specimen's surface by magnetic holders at a fixed distance of 180 mm between them, as shown in Figure 1 (a).

A sampling rate for acquiring the AE features and AE transient waveforms of 10MHz and 5MHz were set in the acquisition system, respectively. Moreover, an amplitude threshold (concerning a reference voltage amplitude of 1μV) of 45 dB and a minimum acquisition frequency equal to 25kHz were applied. It is worth mentioning that the amplitude threshold was selected based on a baseline ramp, where AE signals were detected in a condition where no damage started to propagate, assessing mainly signals related to background noise.

The Vallen AE-Suite Software and Vallen Control Panel (R2017.0504.1) were used to acquire and record the assessed AE data.

3. Acoustic emission post-processing analysis

The acoustic emission raw data of specimen S1 at the first 5000 cycles and the ninth bath of cycles (40000 – 45000) are shown in Figures 3 (a) and (b), respectively.

As shown in Figure 3 (a), the AE amplitude values are very spread during the whole group of cycles with a higher density of signals between 45 to 50 dB and an amount of AE signals around 78000 was recorded. Drawing attention to Figure 3 (b), other areas with a high density of AE signals can be observed. A wavy behaviour was observed in the region between 45 – 60 dB, and a signal's high-amplitude group was noticed at around 70 dB during this batch of cycles. Almost the same amount of AE hits was recorded in this group, about 70000.

No further conclusions can be taken from this raw data. At this point, it is hard to accurately understand if still there are AE signals related to background noise, friction or only hits corresponding to damage initiation and propagation. So, it is crucial to implement an efficient post-processing methodology.

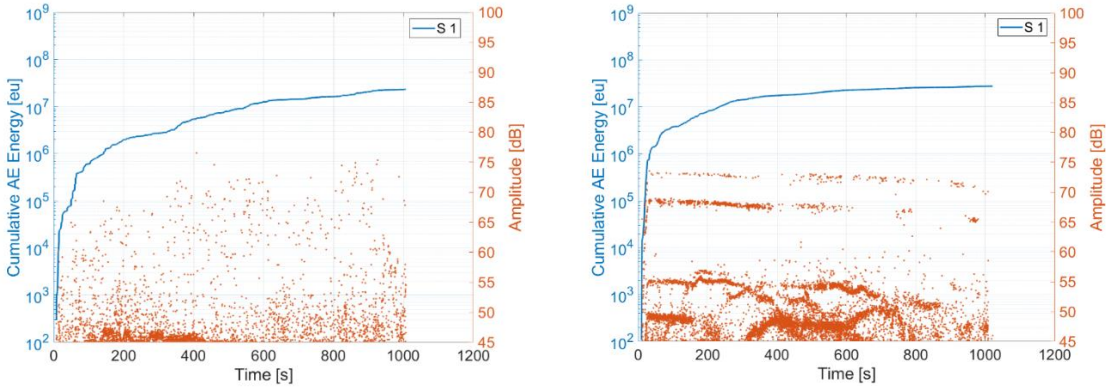

(a) (b)

Figure 3: Specimen's S1 raw data at (a) 0 – 5000 cycles and (b) 40000 – 45000 cycles.

3.1 Classification and Clustering procedure

First, a selection of the most relevant AE features that can be used for the clustering procedure was done by applying the Principal Component Analysis (PCA). Time-domain (Amplitude, Duration, Energy, Rise Time and Counts) and Frequency-domain features (Peak frequency and Centroid frequency) of each recorded waveform were used as input for the PCA, whose calculation procedure is summarized in [9].

In general lines, the PCA is a multivariable data reduction method by creating new minimally correlated features called principal components and forming a symmetric covariant matrix. From the most significant principal component analysis and the variability of the related data, it is possible to determine the main features to increase the clustering procedure's efficiency, as seen in Figure 4. The PCA analysis made it possible to select the duration, energy and frequency as the primary input features for the unsupervised ANN clustering procedure based on creating a 2D topological map that classifies the data using neighbourhood functions (SOM algorithm), as described in [10].

Only by using the SOM it is not possible to divide the classified data into groups, so an additional k-means iterative algorithm was applied. The optimal number of clusters was determined by a combined evaluation of the performance of different indexing criteria such as Davies-Bouldin, Silhouette, and Calinski-Harabasz. An optimal number of 5 clusters was given after the analysis, as seen in the last graph of Figure 4.

Figure 5 shows the specimen S1 at the ninth block of cycles (40000 – 45000) after the clustering procedure. As can be observed, the wavy behaviour was well divided into two main clusters (3 and 4) that present different frequency signatures (cluster 3 – around 150 kHz and cluster 4 – about 100 kHz). The AE hits concentrated in the region of high amplitude values (approximately 70 dB) were grouped in a single cluster (number 5 – colour pink) and present frequency values around 100 kHz, and the highest values of cumulative energy highlighting the direct relationship between amplitude and energy values as stated in [6].

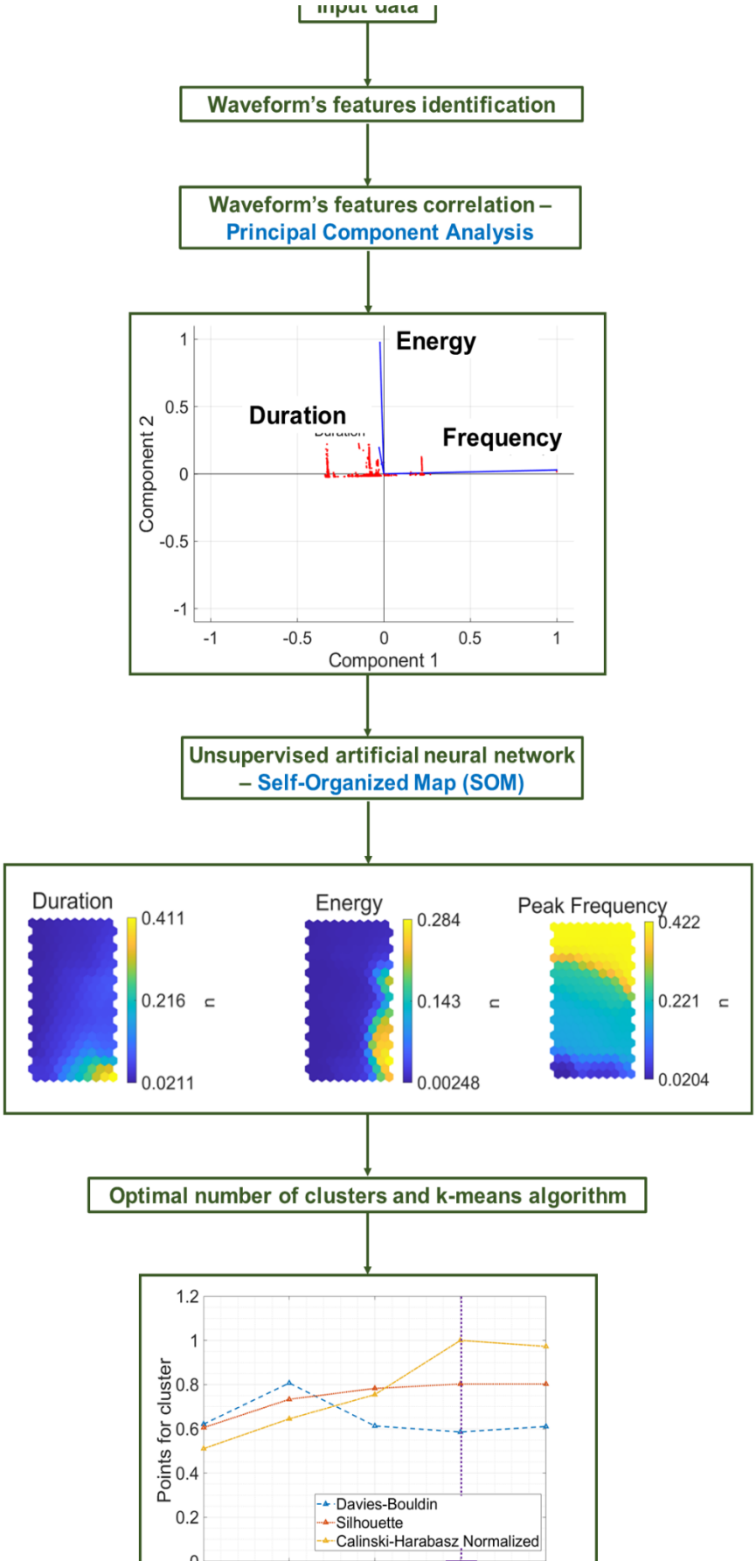

Fig. 4: AE clustering and classification procedure.

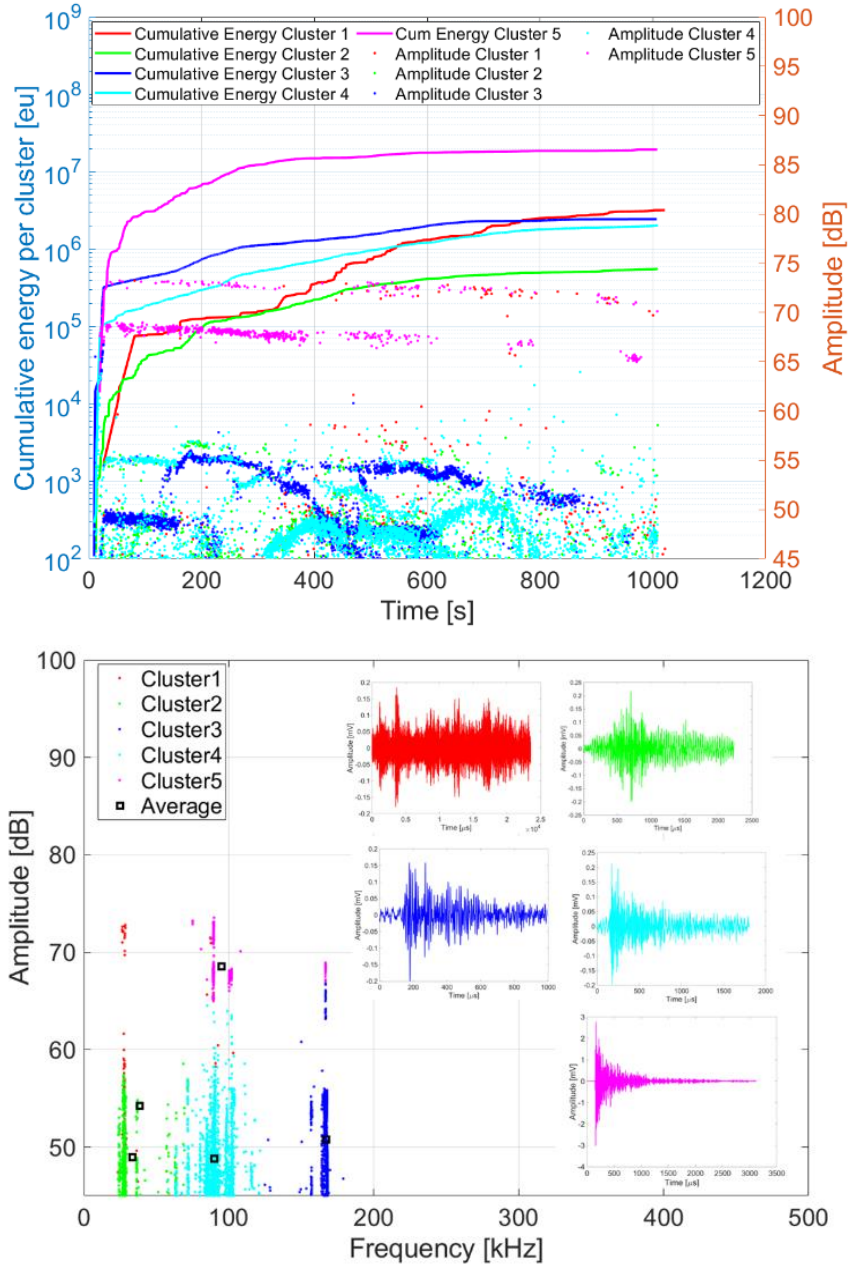

Fig. 5: Specimen S1 at 40000 – 45000 cycles after clustering procedure. (a) Cumulative energy and amplitude values of the clusterised AE data and (b) Frequency signature of each created cluster.

Clusters 1 and 2 instead are very scattered during the whole block of cycles and present the lowest frequency values around 50 kHz. Even if cluster 1 presents high amplitude values, it can be associated with noise or some friction during the tests due to its noisy representative shape shown in Figure 5 (b). So, the main representative clusters that can be used for further analysis are clusters 3, 4 and 5, with frequency signatures in the range from 80 to 150 kHz for the specific studied adhesive. Nonetheless, further research still has to be done to link better the possible damage mechanisms observed during the fatigue crack growth cycles and each classified cluster. It is worth mentioning that similar clustering results were found for specimen S2.

4. DIC, visual evaluation and AE final results

The visual evaluation and DIC crack length measurements obtained during the monotonic ramps for specimens S1, and S2 are shown in Figures 6 (a) and (b). Their results were also compared with the total cumulative energy obtained during the entire fatigue crack growth tests with a total of about 50000 and 100000 cycles for specimens S1 and S2, respectively. Figures 6 (c) and (d) show the total number of hits and the cumulative number of counts for the tests.

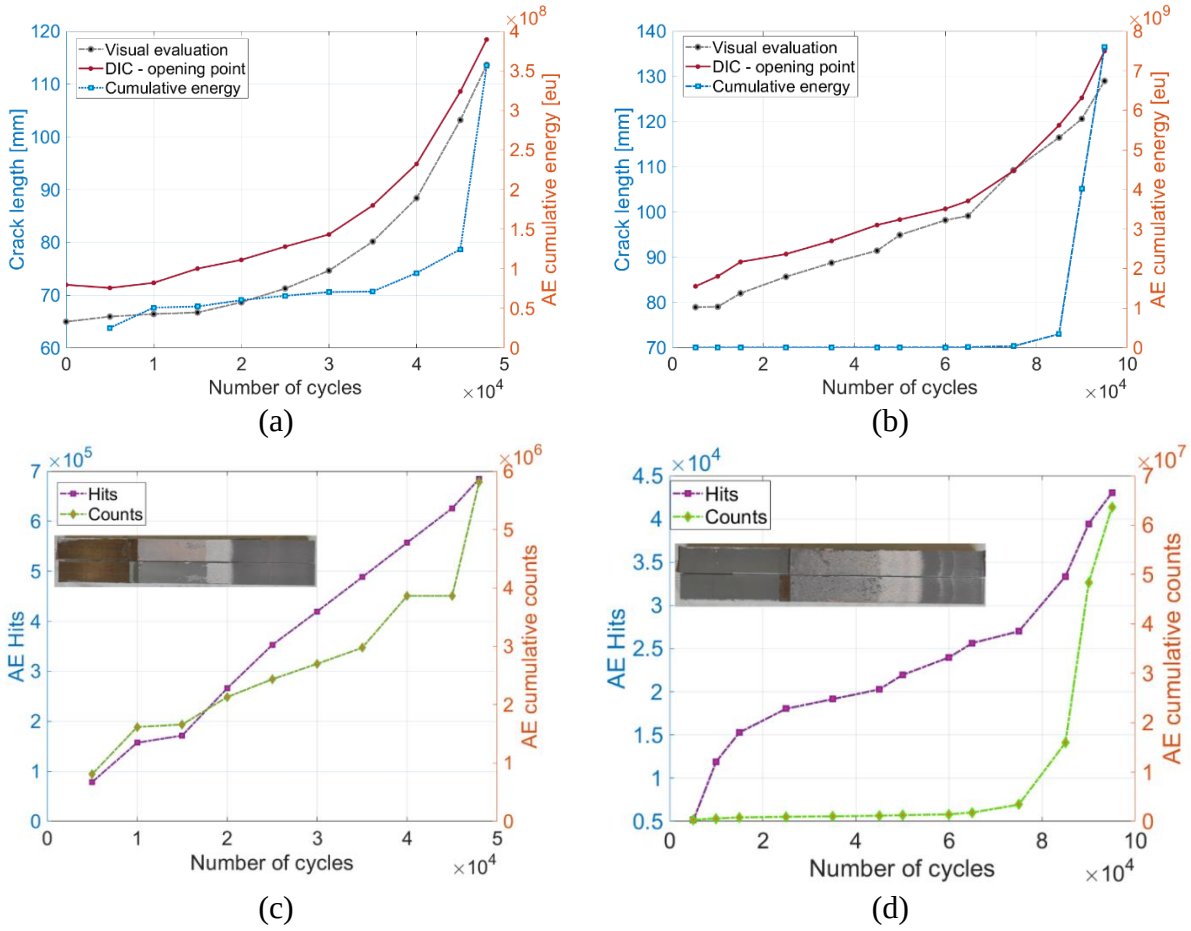

Figure 6: Comparison between DIC, visual evaluation crack length measurements and AE cumulative energy for specimens: (a) S1 and (b) S2, and cumulative hits and counts versus the number of cycles also for specimens: (c) S1 and (d) S2.

First, it is essential to mention that the main difference between the specimen's total number of cycles can be associated with the interfacial failure that occurred in specimen S1 compared to the cohesive failure observed in specimen S2. This can also explain the higher cumulative number of counts obtained for specimen S2, in which waveforms were observed with increased duration and, consequently, the number of counts (number of times that the waveform crosses the threshold) at the last blocks of cycles.

Another difference observed between both specimens is that the cumulative energy of specimen S2 is higher than specimen S1, as observed by S. T. de Freitas et al. 2018 [11]. They observed that the DCB adhesively bonded joints testes under quasi-static mode I that had obtained interfacial failure presented lower cumulative energy than those that underwent a cohesive failure.

As observed in Figures 6 (a) and (b), the crack length measured by the visual evaluation and DIC increase with the number of clusters. The DIC results represents the onset of the plasticisation within the adhesive layer, while the visual evaluation measured the crack-tip position. It was also observed that the cumulative energy of both specimens is almost constant for the whole test and

presents a huge increase next to the last stages of the tests when a high-speed crack propagation was observed. So, the cumulative acoustic emission energy can be useful to identify the fatigue ending the life of the specimens independently of the failure type.

5. Conclusions

This work aimed to study a methodology for acoustic emission clustering and classification of mode I fatigue crack growth within adhesively bonded joints. Moreover, a comparison between the crack growth measured by DIC, visual evaluation and AE features such as the cumulative energy. The main conclusions could be obtained:

- The proposed clustering procedure was able to classify the AE waveforms based on three main features: duration, energy and frequency. Suggesting that some groups can be associated with noise and/or friction. However, further studies should be pursued to understand better the damage mechanisms within the adhesive layer and the AE features;
- High cumulative energy was observed in the specimen that underwent a cohesive failure;
- A massive increase in the AE cumulative energy was observed at the final stages of the fatigue crack growth tests, a promising feature to identify high-speed crack propagation of the joints before its complete failure.

6. References

[1] M. D. Banea, L. F. M. Da Silva, R. D. S. G. Campilho, and C. Sato, "Smart adhesive joints: An overview of recent developments," *J. Adhes.*, vol. 90, no. 1, pp. 16–40, 2014.

[2] S. K. Dwivedi, M. Vishwakarma, and P. A. Soni, "Advances and Researches on Non Destructive Testing: A Review," *Mater. Today Proc.*, vol. 5, no. 2, pp. 3690–3698, 2018.

[3] J. Weiland, M. Luber, R. Seewald, A. Schiebahn, R. Engelbrecht, and U. Reisgen, "Structural health monitoring of adhesively bonded joints: Proposing a new method by use of polymer optical fibers," *Procedia Struct. Integr.*, vol. 28, no. 2019, pp. 1249–1257, 2020.

[4] G. Galanopoulos, D. Milanoski, A. Broer, D. Zarouchas, and T. Loutas, "Health Monitoring of Aerospace Structures Utilizing Novel Health Indicators Extracted from Complex Strain and Acoustic Emission Data," *Sensors*, vol. 21, no. 17, p. 5701, 2021.

[5] M. Carboni and A. Bernasconi, *Acoustic Emission Based Monitoring of Fatigue Damage in CFRP-CFRP Adhesive Bonded Joints*, vol. 127. Springer International Publishing, 2021.

[6] J. A. Pascoe, D. S. Zarouchas, R. C. Alderliesten, and R. Benedictus, "Using acoustic emission to understand fatigue crack growth within a single load cycle," *Eng. Fract. Mech.*, vol. 194, no. March, pp. 281–300, 2018.

[7] A. Bernasconi, R. A. A. Lima, S. Cardamone, R. B. Campbell, A. H. Slocum, and M. Giglio, "Effect of temperature on cohesive modelling of 3M Scotch-Weld™ 7260 B/A epoxy adhesive," *J. Adhes.*, vol. 96, no. 1–4, pp. 437–460, 2020.

[8] R. A. A. A. A. Lima, R. Perrone, M. Carboni, and A. Bernasconi, "Experimental analysis of mode I crack propagation in adhesively bonded joints by optical backscatter reflectometry and comparison with digital image correlation," *Theor. Appl. Fract. Mech.*, vol. 116, no. July, p. 103117, Oct. 2021.

[9] C. Barile, C. Casavola, G. Pappalettera, and P. K. Vimalathithan, "Multiparameter approach for damage propagation analysis in fiber-reinforced polymer composites," *Appl. Sci.*, vol. 11, no. 1, pp. 1–14, 2021.

[10] R. A. A. Lima, M. Drobiazko, A. Bernasconi, and M. Carboni, "On crack tip localisation in quasi-statically loaded, adhesively bonded double cantilever beam specimens by acoustic emission," *Theor. Appl. Fract. Mech.*, vol. 118, no. February, p. 103286, 2022.

[11] S. Teixeira de Freitas, D. Zarouchas, and J. A. Poulis, "The use of acoustic emission and composite peel tests to detect weak adhesion in composite structures," *J. Adhes.*, vol. 94, no. 9, pp. 743–766, 2018.